Genome Biology

RESEARCH

Open Access

Contribution of homoeologous exchange to domestication of polyploid *Brassica*

Tianpeng Wang[1,2,3], Aalt D. J. van Dijk[3], Ranze Zhao[1], Guusje Bonnema[2*] and Xiaowu Wang[1*]

*Correspondence:
guusje.bonnema@wur.nl;
wangxiaowu@caas.cn

[1] State Key Laboratory of Vegetable Biobreeding, Institute of Vegetables and Flowers, Chinese Academy of Agricultural Sciences, Beijing, China
[2] Plant Breeding, Wageningen University and Research, Wageningen, The Netherlands
[3] Bioinformatics Group, Wageningen University and Research, Wageningen, The Netherlands

Abstract

Background: Polyploidy is widely recognized as a significant evolutionary force in the plant kingdom, contributing to the diversification of plants. One of the notable features of allopolyploidy is the occurrence of homoeologous exchange (HE) events between the subgenomes, causing changes in genomic composition, gene expression, and phenotypic variations. However, the role of HE in plant adaptation and domestication remains unclear.

Results: Here we analyze the whole-genome resequencing data from *Brassica napus* accessions representing the different morphotypes and ecotypes, to investigate the role of HE in domestication. Our findings demonstrate frequent occurrence of HEs in *Brassica napus*, with substantial HE patterns shared across populations, indicating their potential role in promoting crop domestication. HE events are asymmetric, with the A genome more frequently replacing C genome segments. These events show a preference for specific genomic regions and vary among populations. We also identify candidate genes in HE regions specific to certain populations, which likely contribute to flowering-time diversification across diverse morphotypes and ecotypes. In addition, we assemble a new genome of a swede accession, confirming the HE signals on the genome and their potential involvement in root tuber development. By analyzing HE in another allopolyploid species, *Brassica juncea*, we characterize a potential broader role of HE in allopolyploid crop domestication.

Conclusions: Our results provide novel insights into the domestication of polyploid *Brassica* species and highlight homoeologous exchange as a crucial mechanism for generating variations that are selected for crop improvement in polyploid species.

Background

Polyploidy, referring to either the duplication of a single genome (autopolyploidy) or to the combination and doubling of two or more different genomes (allopolyploidy), has long been recognized as a major force in plant evolution and speciation [1–4]. All seed plants have undergone at least one polyploidization process during their evolutionary history [5–7]. Polyploidy is prevalent among domesticated crops, some of which have even experienced multiple rounds of polyploidization [8, 9]. As a result of this

association, polyploidy has long been proposed as a crucial factor in crop domestication [10, 11]. Such important role of polyploidy is thought to result from the rapid and dynamic changes in genomes that occur at the beginning of polyploid formation [12, 13]. Following genome merging and doubling, polyploidization leads to dramatic "genomic shocks" with large numbers of structural variations (SV) being a prominent feature, which may give rise to novel phenotypes and thus provide substrates for natural selection and successful domestication [14–16]. Understanding mechanisms of polyploidy and its various consequences that lead to successful domestication is of fundamental importance for a full appreciation of its potential.

One causal mechanism of the "genomic shock" early in the formation of polyploids is the occurrence of homoeologous exchange (HE) between the two constituent subgenomes, which has been increasingly reported in recent years [17–19]. HE is a mechanism unique to allopolyploids and relates to the exchange of chromosome segments via crossover formation between homoeologous chromosomes [20, 21]. While the HE mechanism is inherently reciprocal, the recombinant chromatids resulting from an initial HE event are typically not segregating into the same resulting gamete. Instead, they are often identified as unbalanced exchanges or duplication–deletion events, wherein one gene is entirely replaced by a duplicate of its homoeolog from the other subgenome [19]. Although exchanges that involve homoeologs switching places with each other can also become stable through self-pollination and selection, their detection via sequencing methods poses challenges [17, 22]. HEs are extremely prevalent in both newly synthesized and established allopolyploid plants, including wheat [23], rice [24, 25], rapeseed [26–29], and peanut [30], suggesting that HEs likely contribute to plants escape from genetic bottlenecks during the initial stage of polyploidization and have been selected during species diversification and crop domestication. Gaining a deeper understanding of homoeologous exchange and its consequences at the genome level has the potential to catalyze new breakthroughs to improve the diversity of polyploid crops.

Understanding what factors cause homoeologous exchange requires tracing back to the meiotic pairing process at the onset stage of allopolyploid species formation [31]. After merging and doubling divergent genomes into the same nucleus, the immediate challenge for the newly formed allopolyploids is to stabilize their meiotic regulation process, as their inherited homoeologous chromosomes may pair and recombine between each other, which could result in abnormal segregation and aneuploidy [17, 32, 33]. In well-established allopolyploid species, HE events are relatively stabilized. As aneuploidy is rare in such polyploids, mechanisms to control chromosome pairing likely exist in polyploids, therefore, allowing them to behave genetically as diploids during meiosis [31]. Genetic research revealed that pairing control mechanisms are attributed to either specific genetic loci, such as *Ph1* in polyploid wheat [34], *BnaPh1* and *PrBn* in *Brassica napus* [35, 36], or due to the intrinsic homoeologous genome divergence [29].

HE-induced chromosome segment reshuffling may induce or contribute to dramatic genomic and transcriptomic changes, therefore affecting the phenotypic variations of plants [17]. Following chromosome segregation over time, HEs can result in one of the DNA fragments replacing the corresponding homoeologous regions and becoming fixed. This process would consequently lead to a segmental allopolyploid genome that contains a mix of auto- and allopolyploid segments [15, 37, 38]. By using synthetic

allopolyploids, previous research has shown that HE affects gene expression within HE regions through dosage effects, resulting in significant alternations in the overall expression levels of homoeologous gene pairs [39, 40]. Interestingly, genes in HE regions were shown to be associated with diversity in many important trait in polyploid crops, including flowering time [41, 42], leaf shape and color [27, 30], seed glucosinolate content [29], and disease resistance [38], suggesting significant influence of HEs on important traits. However, despite the prevalence of HEs and their potential association with phenotypes, much is still unknown about the role of HEs in trait diversification and crop domestication.

Brassica napus (AACC, $2n=4x=38$) is a relevant target species to study the impact of homoeologous exchange on crop domestication because of its worldwide cultivation and adaptation in diverse climate zones, and as it possesses some favorable attributes including the availability of well-established genomes, genetic transformation, and ease of resynthesis [28, 43, 44]. *B. napus* is a recent allopolyploid species resulting from the interspecific hybridization between two closely related diploid species *B. rapa* (AA, $2n=2x=20$) and *B. oleracea* (CC, $2n=2x=18$), according to the "triangle of U" [45]. Within the species, it comprises three diverse morphotypes, including oil-type *B. napus* subsp. *oleifera* (rapeseed or oilseeds), tuber-type *B. napus* subsp. *rapifera* (swede or rutabaga), and leafy-type *B. napus* subsp. *pabularia* (Siberian kale or leaf rape) [28, 46]. The oil types can be further divided into winter, spring, and semi-winter ecotypes based on different needs of vernalization, as a result of artificial selection in different regions of the world [47]. Our recent research has shown that *B. napus* derived from the hybridization of European turnip of *B. rapa* and wild *B. oleracea*, and that interploidy introgression is prevalent during its domestication history [48]. Furthermore, many in-depth studies have been conducted in *B. napus* regarding the mechanisms and impacts of HEs. The HEs phenomenon was first reported in synthetic *B. napus*, dating back at least to 1995 [49], and later the association of HE with flowering time diversification was also established [27, 41, 49, 50]. Recently, the availability of large amounts of genomic data has made it possible to study the impact of HEs of polyploid species at the population level and sequencing depth-based method has been develop for detecting HE in *B. napus*. These studies utilizing the whole-genome resequencing data have revealed that HEs have much higher frequency in the germplasm and are the main source of gene presence-absence variation in *B. napus* [29, 38]. However, the impact of the variations resulting from HEs on crop domestication has not yet been studied in detail.

In this paper, we performed a comprehensive study of the prevalence and the role of homoeologous exchanges in the domestication of allopolyploid *B. napus* crops. We explored genomic features and patterns of HEs among the different morphotypes and ecotypes and examined their direct impacts on gene expression changes. We then qualified the impact of HEs on the diversification of the different morphotypes in *B. napus* by using flowering time variation as a clear example. In addition, we assembled a reference genome of the swede morphotype which confirmed the "segmental allopolyploid" character of its genome and allowed to investigate the potential impact of HE on tuberous organ formation. Finally, we analyzed the HE status in the related polyploid *B. juncea* species, also characterized by a diversity of morphotypes, and showed that HEs play a generic role in crop domestication and diversification.

Results

Prevalence of homoeologous exchanges in the domesticated *Brassica* napus

To fully characterize the homoeologous exchange (HE) events in the domestication history of *Brassica napus*, we collected publicly available whole genome resequencing data of 260 accessions representing all various morphotypes and ecotypes, including swede, Siberian kale, winter rapeseed, spring rapeseed, and semi-winter rapeseed. In addition, we included the resequencing data of 8 accessions each of European turnip (*B. rapa*) and wild-type *B. oleracea*, which were combined to represent the in silico ancestry of *B. napus* and used as a control group for subsequent analyses (Additional file 2: Table S1). We first aimed to understand the phylogenetic relationships between different morphotypes in the domestication history of *B. napus*. With the in silico progenitor accessions as the outgroup, we found that the phylogenetic clustering clearly resolved five groups plus the outgroup, which are highly consistent with different morphotypes and ecotypes (Fig. 1; Additional file 1: Fig. S1). In particular, the phylogeny revealed that the

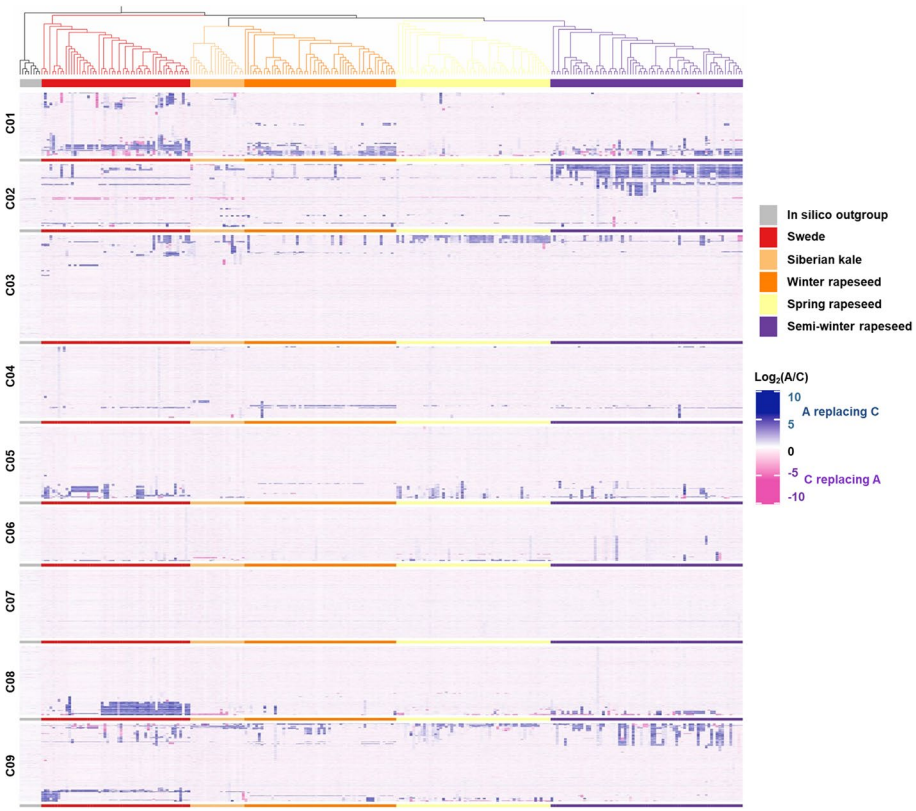

Fig. 1 The occurrence of homoeologous exchanges between A and C genome during the domestication of *Brassica napus*, as indicated by C genome coordinate. A total of 260 accessions of *B. napus*, representing diverse morphotypes and ecotypes, are ordered according to their phylogenetic relationships, with in silico progenitors as the outgroup. The group names are indicated as the colored bars at the bottom. The homoeologous exchange values represent $\log_2$-transformed mapping density ratios of the homoeologous gene pairs, with the blue and purple components representing the coverage abundance of the A and C genome, respectively. The homoeologous gene pairs are plotted on the Y axis as C genome chromosomes ordered from C01 to C09 and on the X axis based on the phylogenetic relationships of all accessions. Expanded views of each chromosome are available in Supplementary figures S8-S16. Detailed homoeologous relationships between the A and C genomes are presented in Supplementary Figure S3

morphotypes of swede and Siberian kale (used as vegetable and fodder) were domesticated before rapeseed (oil crop), with the hypocotyl-root tuber swede as the basal clade in the phylogeny. With regard to rapeseed, the winter ecotype was the basal type, from which spring and semi-winter ecotypes diversified.

Homoeologous exchange events were assessed by calculating the A-C ratio of read coverage depth of resequencing data from 260 *B. napus* accessions and the in silico control accessions on the combined reference genome of the diploid ancestral species (*B. rapa*, A genome; *B. oleracea*, C genome) (Additional file 1: Fig. S2). We identified 31,456 homoeologous gene pairs, which were used as anchors to represent the homoeologous regions between the A and C genomes (Additional file 1: Fig. S3; Additional file 2: Table S2). The $\log_2$-transformed mapping density ratio values of the homoeologous gene pairs were designated as HE values and were visualized across chromosomal sequences based on the gene order of the C genome (Additional file 1: Figs. S4, S5). No HE regions were detected in the 64 in silico combinations of ancestral accessions used as negative control (Additional file 1: Fig. S6). As a positive control, we also included sequencing data from eight rapeseed accessions from which reference genomes had previously been assembled and confirmed the presence of HE in these accessions [44] (Additional file 1: Fig. S7). Those results indicate the reliability of the HE identification method.

A total of 260 accessions used in this study all exhibited substantial HE segments of different sizes, which strongly indicate the prevalence of HE in the *B. napus* germplasm (Fig. 1, Additional file 1: Figs. S8-S16, Additional file 2: Table S3). The length of HE fragments where A replaced C ranged from 13.1 kb to 16.2 Mb, with an average length of 763.3 kb. One of the swede accessions (3052GSS) showed the most HE events, with 36.3 Mb (6.7%) of the C genome replaced by homoeologous A genome segments. On the other hand, in accessions where C replaced A, HE fragments ranged from 10.3 kb to 4.66 Mb, with an average length of 204.1 kb. A semi-winter rapeseed accession (R5085) had the highest number of HEs, replacing 7.69 Mb (2.54%) of the A genome with homoeologous C fragments. Besides, some HEs appeared only in a single accession, absent in other phylogenetically related ones, suggesting their recent emergence and that the occurrence of HE is ongoing. When considering the extent of coverage across the whole genome, approximately 37.1% of the C genome and 39.8% of the A genome was affected by HE in at least one accession. Notably, some genomic hotspot areas exhibited HEs in the majority of the accessions, such as C01, C09, and their homoeologous A regions. In these regions, HEs can occur with opposite directions, forming AAAA structures in some accessions and CCCC structures in others, indicating the variability and ongoing process of HEs in these tetrasomic regions during the recent domestication process (Additional file 1: Figs. S8, S16). In summary, these results clearly show that HEs are extremely prevalent in *B. napus* populations, suggesting a likely role in their adaptation and domestication into diverse crops and ecotypes.

Genomic and transcriptomic features of HEs

Building on the initial catalog of HEs, we then turned our attention to an investigation of features describing the observed HEs patterns. Firstly, HEs exhibited an uneven distribution across the chromosomes in the *B. napus* population. Genomic characterization of all HE events in the 260 accessions revealed that certain regions of the chromosomes

are favored for the presence of HE (Fig. 1). Alignment of those HEs to the relative position of centromere to telomeres showed that HEs tend to be located in the distal third of chromosome arms, which is also a region of high gene density and high recombination rates (Fig. 2A). Secondly, HEs tend to occur in a biased direction between the A and C genomes. We found that on average, each accession contains 16 instances in the case of A chromosome segments replacing C chromosome segments, significantly higher than the 7 instances in the opposite direction (Mann–Whitney tests, $P < 2.2e-16$) (Fig. 2B). When assessing the accumulated size of replaced segments within accessions, HEs of A replacing C had a much higher average length of 12.1 Mb, compared to 2.5 Mb for C replacing A (Fig. 2C). These findings indicate a prevailing dominance of the A subgenome over the C subgenome in the context of HE. Thirdly, the biased direction of HEs was observed to vary among different morphotypes. HEs of A replacing C were significantly higher than C replacing A in most morpho- and ecotypes, with the exception in the Siberian kale group of lower HEs frequency in both directions (Fig. 2D). Additionally, the occurrence of HE differed among the homoeologous chromosomes. Chromosomes C01 and C02 showed two of the highest amounts of accumulative HE lengths among all accessions, which correlated with their high collinear relationship with their homoeologous A01 and A02 chromosomes, respectively (Fig. 2E; Additional file 1: Figs. S3, S8 and S9). On the contrary, chromosomes with lower collinearity, such as C06 and C07,

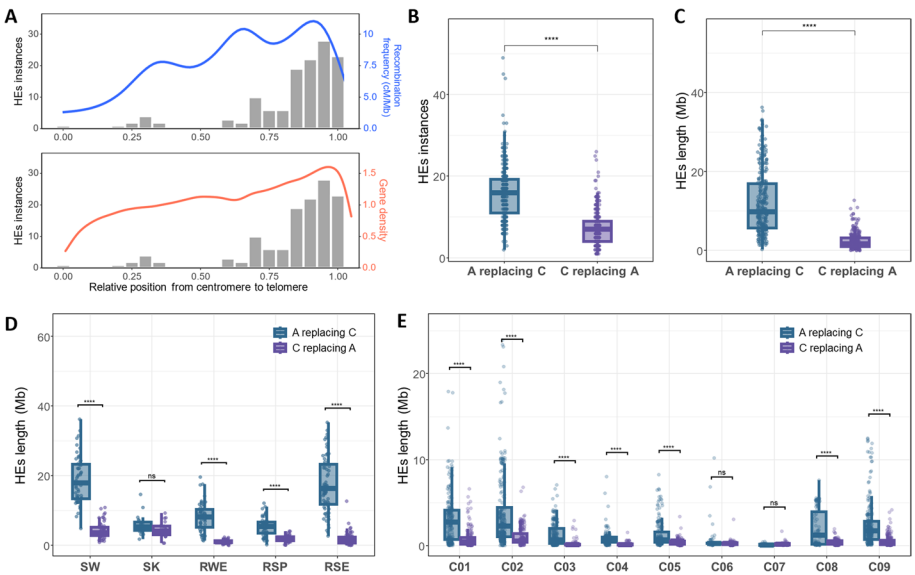

Fig. 2 Genomic distribution and characteristics of homoeologous exchanges. **A** Distribution of HEs across the relative chromosome positions from centromere to telomere, with indications of recombination frequency and gene density. The histogram reflects the cumulative count of HEs in each bin. Recombination frequency (cM/Mb, shown in blue) and gene density (% genic sequence, shown in red) are illustrated along the average chromosome arm. **B** Comparison of HE events between chromosomal segments of "A replacing C" and "C replacing A" in *B. napus* populations, as measured by HE cases from each accession. **C** Comparison of HE events, measured by the accumulative genome size of the replaced segments in each accession. **D** Comparison of accumulative genome size for HE events within different *B. npaus* groups: Swede (SW), Siberian kale (SK), Winter rapeseed (RWE), Spring rapeseed (RSP), Semi-winter rapeseed (RSE). **E** Distribution and comparison of the accumulative genome size of HE events indicated by different C chromosomes. Mann-Whitney tests were used to assess significance between HE directions with asterisks indicating significance level. $^{***}P < 0.001$, $^{**}P < 0.01$, $^{*}P < 0.05$, $^{ns}P > 0.05$

exhibited much lower HE events with their homoeologous A chromosomes (Additional file 1: Figs. S13, S14). In general, these genomic characteristics of HEs provide insights into their preferences within specific regions of the genome and for distinct morpho- and ecotypes.

The direct effect of HE on genes is that it could lead to duplication or deletion of one of the homoeologs, potentially leading to expression changes for both genes and homoeologous gene pairs in allopolyploids [39, 40, 51]. We then investigated the effect of HEs on expression changes of HE-affected genes in *B. napus* populations using public data from 119 accessions [46]. We selected accessions where both RNA and DNA were extracted from young leaves, allowing us to quantify the occurrence of HE and the expression of HE-affected genes at the same time. HE events were again found to be prevalent in those 119 *B. napus* accessions (Additional file 1: Fig. S17). The further analysis revealed that the expression levels of the replacing genes were significantly elevated, likely due to the presence of additional gene copies created by HEs (Additional file 1: Fig. S18A, S18B). Additionally, HEs were generally associated with total expressional alterations of their homoeologous gene pairs. For those homoeologous genes with different expression levels in the pre-HE status, the post-HE expression of the higher expressed homoeologs (AA or CC) tended to show increased expression compared to the HE-free homoeologs (AC) (Additional file 1: Fig. S18C, S18E). In contrast, the post-HE expression of the lower expressed homoeologs (AA or CC) tended to show decreased total expression compared to the HE free homoeologs (AC) (Additional file 1: Fig. S18D, S18F). In general, HEs were associated with total expressional alterations of their homoeologous gene pairs, but those changes would depend on the differential expression levels between A and C genes in their initial status. Those expressional changes resulting from HEs could lead to potential functional diversification in *B. napus* populations.

Selection of HEs in the morphotype domestication

Given the widespread occurrence of homoeologous exchanges among the sampled accessions, it is hypothesized that in the domestication process, accessions with the favored genomic variations resulting from HE were selected, leading to the fixation of different HE patterns among different populations (Additional file 1: Fig. S19). Our objective was then to investigate the potential contributions of HE patterns to the domestication of diverse morphotypes and ecotypes in *B. napus*. We calculated HE patterns per morpho/ecotype by determining the average value across the genome of all corresponding accessions. The 64 in silico ancestral accessions were utilized as a control for comparisons of morpho/ecotype HE patterns.

Our findings revealed distinct patterns of homoeologous exchanges across various morphotypes and ecotypes of *B. napus*, with certain patterns exclusive to specific populations (Fig. 3, Additional file 2: Table S4). Among the morphotypes, swede exhibited the highest incidences of HE events, with 20 distinct signals covering 20.3 Mb of the C genome at the population level, particularly involving homoeologous regions such as C01-A01, C08-A09, and C09-A10. Those events were predominantly in the direction of A genome segments replacing those of C genome, which involved 1188 homoeologous gene pairs specific to this morphotype (Additional file 1: Fig. S20A). In contrast, the Siberian kale group displayed a smaller number of

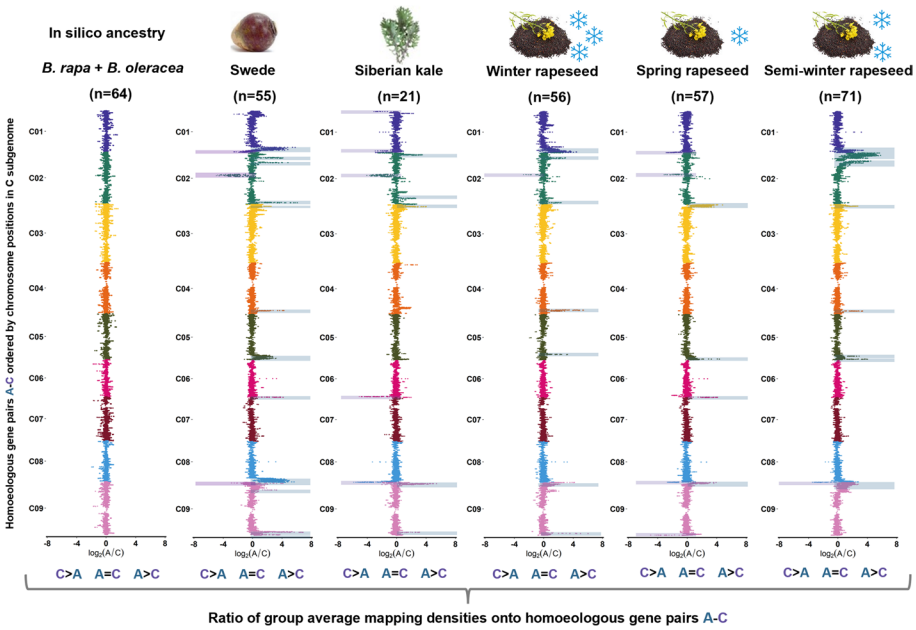

Fig. 3 Visualization of group-level homoeologous exchange patterns across various morphotypes and ecotypes in *Brassica napus*. HE value is denoted as $\log_2$-transformed values of ratios of mapping densities of whole-genome sequences onto homoeologous A/C gene, ordered by chromosome number and position in C genome. The number of accessions within each morphotype is denoted as "n". Group-level HE is determined by calculating the mean value of HE ratio for all accessions in this group, using a sliding window of 5 genes with steps of 2 genes across the genome. A HE event occurs when log2-transformed values deviate from zero, indicating the occurrence of homoeologous gene pair replacement, which leads to either AAAA or CCCC genome structures represented by blue and purple regions, respectively. Equivalence of log2-transformed values to zero indicates an unaltered genome structure of AACC

HE group signals, with a significant proportion involving the replacement of the A genome with the C genome (8 signals corresponding to 205 gene pairs) (Additional file 1: Fig. S20B). The various rapeseed ecotypes displayed a moderate level of HE signals, along with numerous ecotype-specific patterns. Notably, a prominent large HE segment involving the "A replacing C", spanning up to 7.3 Mb, was identified on homoeologous chromosome C02-A02 in the semi-winter rapeseed group, similar to the findings of accessions from the pan-genome study of *B. napus* [44], indicating the widespread presence of this large segment in the semi-winter rapeseed ecotype. Additionally, some HE patterns showed opposite directions in different groups. HEs involving "A replacing C" were observed on chromosome C08 in swede morphotypes, whereas an inverse pattern of "C replacing A" was detected in both Siberian kale and semi-winter rapeseed groups. This indicates a set of genes from the A genome may be favored in swede, while in other morphotypes, their homoeologs from the C genome are favored (Fig. 3). In summary, our results provide evidence for the selection of HEs during morphotype domestication. Those group-level HE patterns observed among diverse morphotypes and ecotypes suggest potential roles in their differentiation and adaptation to local environments throughout the domestication process.

Contribution of HEs to the flowering-time diversification

We then selected representative HEs events among various morphotypes and ecotypes to investigate their functional significance to phenotypic changes during *B. napus* domestication. One of the major traits for plants adapting to various environments worldwide is flowering-time regulation, which synchronizes plant development with the local climate conditions [52]. According to the different vernalization requirements, *B. napus* has diversified into three different ecotypes (winter, spring, semi-winter). Our approach focused on genes located within HE regions selected for different populations, as the high degree of this structure variation observed within the population is indicative of its adaptive value.

Our examination of HE effects on flowering-time related genes revealed substantial impacts on the diversification of different ecotypes. A comprehensive inspection of 306 Arabidopsis flowering-related genes using the Flowering Interactive Database (FLOR-ID) identified 394 homoeologous gene pairs in *B. napus* (Additional file 2: Table S5) [53]. Among various morphotypes and ecotypes, we detected a total of 57 flowering-related gene pairs affected by HE on the group level, with 38 of them specific to particular morphotypes and ecotypes, suggesting a substantial role for flowering-time related genes in driving the diversification of different ecotypes (Additional file 1: Fig. S21; Additional file 2: Table S6). For instance, a prominent segment of HE, representing the chromosomal segments of A02 replacing C02, was detected in the majority of semi-winter rapeseed accessions (Fig. 3). In this specific HE region, 8 flowering time-related gene of the C subgenome were replaced by their homoeologous genes of the A subgenome, including *COL5.A02-C02* (*CONSTANS-LIKE 5,* 42/71), *VIN3.A02-C02* (*VERNALIZATION INSENSITIVE 3,* 50/71). Similarly, in the spring rapeseed group, we identified HE segments of A replacing C on C03/A03, encompassing gene pairs such as *UBP12.A02-C02* (*UBIQUITIN-SPECIFIC PROTEASE 12* 43/57), *FTIP1.A03-C03* (*FT-INTERACTING PROTEIN 1,* 28/57). These data suggest the potential importance of HE-mediated alterations in flowering genes for rapeseed ecotypes adapting to different growing seasons.

Among the flowering-time genes, *FLOWERING LOCUS C* (*FLC*) homologs were notable, as the three different *FLC* homoeologous gene pairs were impacted by HEs in different groups, resulting in expressional changes (Additional file 1: Figs. S22, S23; Additional file 2: Table S6). Specifically, a distinct HE of A replacing C event on the C09-A10 chromosome segment resulted in the replacement of the *FLC.C09* gene with its homolog *FLC.A10* in all 55 accessions of the swede group (Fig. 4A, C). The swede morphotype, known for its winter-annual flowering behavior requiring extended vernalization [42], exhibited a much delayed flowering time when compared to other groups, with an average of 195 days after sowing (Fig. 4B; Additional file 1: Table S7) [54]. Further exploration of this gene pair across the 119 available accessions, with both genomic and transcriptome data from young leaf [46], confirmed the HEs of *FLC.A10-C09* in all 19 swede accessions (Fig. 4C). Transcriptome analysis from those accessions showed that the expression level of *FLC.A10* was significantly higher in swede accessions than in other groups, whereas the expression of *FLC.C09* remained consistently low across all groups (Figs. 4D and 5E). Besides, the two gene duplicates of *BnaFLC.C09* in *B. napus* were also found to be low-expressed among different groups (Additional file 1: Fig. S24). Notably, the expression of *FLC.A10* exhibited a two-fold increase in the swede group

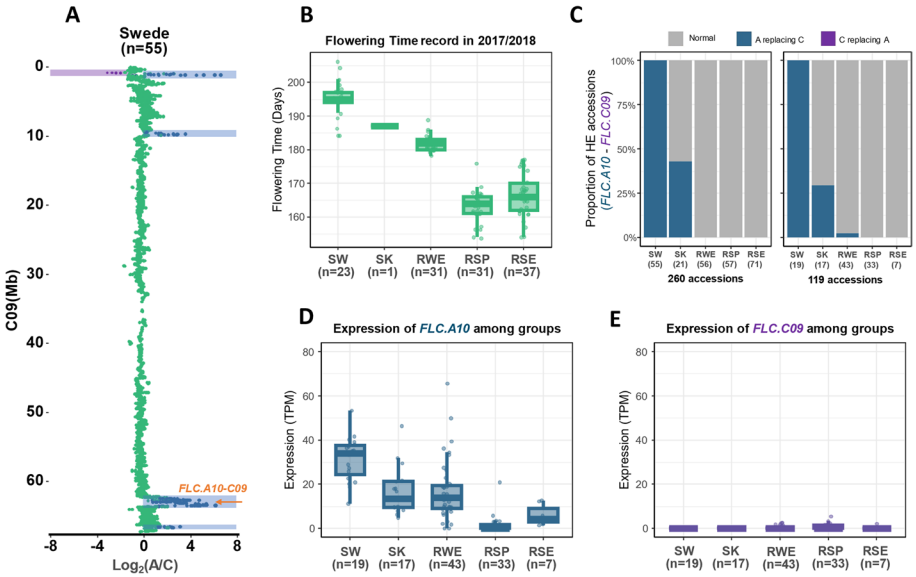

Fig. 4 Impact of homoeologous exchanges on *FLC.A10-C09* gene pair associated with prolonged flowering time domestication in Swede morphotype. **A** Illustration of HE signals based along chromosome C09 for swede morphotype, with the blue color indicating "A replacing C" group signals and purple for "C replacing A". **B** Flowering time record for 123 accessions during the 2017/2018 season, sourced from Wu et al. **C** Analyses of the HE involving the *FLC.A10-C09* gene pair across 260 accessions from this study, and additional 119 accessions from An et al. [46]. The bar plot represents the proportion of accessions that showed HE on *FLC.A10-C09* gene pair within each group. **D**, **E** Expression levels of *FLC.A10* and *FLC.C09* genes in young leaves from 119 accessions. Swede (SW), Siberian kale (SK), Winter rapeseed (RWE), Spring rapeseed (RSP), Semi-winter rapeseed (RSE). The number of accessions in the group is listed between brackets

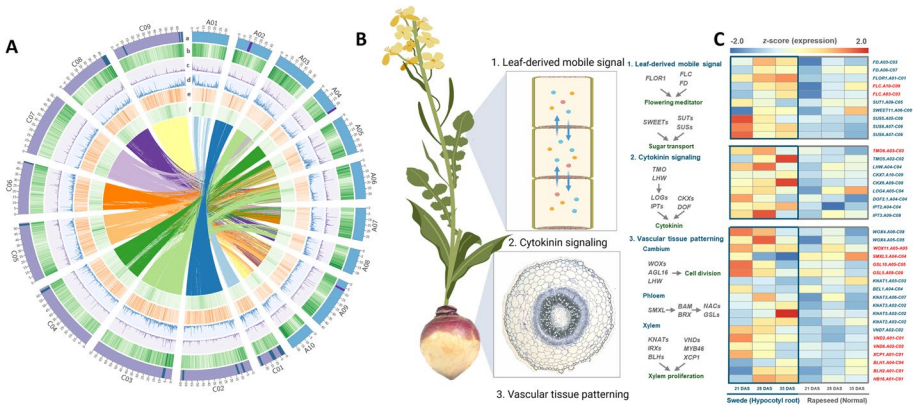

Fig. 5 Homoeologous exchange in swede genome assembly and their involvement in hypocotyl-root development. **A** Genomic features of the swede genome assembly. (a) Distribution along the assembled 19 chromosomes (A01 to A10, and C01 to C09), with HE events of either A replacing C regions denoted as blue and C replacing A regions denoted as purple. Gene density track (b). Expression of annotated gene in leaf (c) and root (d) as measured by FPKM. Density of transposon (e) and retrotransposon (f). Lines in the center show the syntenic regions between the A and C genomes. **B** Graph of *B. npaus* swede morphotype and the three main regulatory programs associated with different hypocotyl-root developmental events. **C** Expression profiles of representative gene pairs showing differential expression during hypocotyl-root development between swede and rapeseed. Gene pairs affected by homoeologous exchange are indicated in red. The hypocotyl-root in swede starts to expand approximately 21–28 days after sowing (DAS)

relative to the other two winter ecotypes, Siberian kale and winter rapeseed, which correlated with the gene duplication resulting from the HE. *FLC.A10*, also known as *FLC1*, has been identified in previous studies for its important role in the vernalization requirement in *B. rapa* [55] and *B. napus* [54, 56]. Therefore, the presence of HE in the swede group, leading to the duplication and higher expression of *FLC.A10*, likely contributes to the extended flowering time and prolonged vegetative growth observed in this morphotype. This underscores the potential role of HE in the diversification and domestication of the swede morphotype, highlighting its significance in shaping plant phenotypes.

Involvement of HEs in swede hypocotyl-root domestication

Since the swede morphotype is characterized by its distinct root enlargement trait and has significantly more HEs compared to other morphotypes (Fig. 5A), we then intended to validate these findings by first generating a representative swede reference genome and explored the potential role of HE during hypocotyl root development. We selected a representative swede accession and sequenced its genome using both Nanopore and Illumina platforms, generating 97.3 Gb (~ 100x) and 110.8 Gb (~ 120x) data, respectively (Additional file 2: Table S8). The assembly generated 895 Mb genome size with a contig N50 of 4.3 Mb, further ordered into 19 pseudo-chromosomes utilizing Hi-C data covering 92.6% of the genome (Fig. 5B; Additional file 1: Fig. S25; Additional file 2: Table S9). Genome annotation led to 97,852 protein-coding genes with an average length of 2354.3 base pairs (bp) and 4.62 exons per gene, verified by 97.29% coverage of RNA-seq data (Additional file 2: Table S10). The analysis also revealed 372.56 Mb of transposable elements (TEs), including 15.71% LTR retrotransposons, within the assembled swede genome (Fig. 5B). BUSCO statistics confirmed the high-quality assembly compared to other *B. napus* genomes (Additional file 2: Table S11).

Given the completeness and collinearity of the newly assembled swede genome, we investigated the HE segments in this segmental allopolyploid genome. Investigation of the HE signals using the Nanopore long-read data revealed 17 HE signals, confirming 16 signals previously identified with short reads and uncovering one missed segment on C01 (Additional file 1: Fig. S26). We then compared the collinearity between our assembly and the pseudo-ancestry *B. napus* genome, which is concatenated by *B. rapa* and *B. oleracea* genomes. The results show that our assembled genome has good syntenic relationship with the pseudo-ancestral genome, with one-on-one matches on the majority of chromosome regions, while some inversions also exist (Additional file 1: Fig. S27). We also found that on the chromosome regions where HEs occur, the genomes showed direct collinearity with the replaced ancestral genome. This newly assembled swede genome confirmed previous HE findings based on short-read sequencing.

We next generated time-course gene expression profiles from stages around the tuber initiation timepoint of swede with the non-tuber forming rapeseed as comparison. Analysis of HE ratios identified that 1405 homoeologous gene pairs were affected by HE in the swede accession compared to the rapeseed accession (Additional file 2: Table S12). From the 1405 HE gene pairs, 865 exhibited differential expression during swede hypocotyl development compared to rapeseed (Additional file 1: Fig. S28). This indicates that the HE gene pairs are enriched for differentially expressed genes (Fisher's exact test, $P < 0.01$), suggesting HE might play a role in the swede tuberization process. HEs can

lead to changes in gene expression primarily through the replacement of gene copies, which may alter the overall transcriptional output of affected gene pairs. This is particularly relevant for genes involved in key developmental processes. According to the previous findings on mechanisms underlying the tuberous organ development, we focused on three essential and well-characterized developmental programs: leaf-derived mobile signal transduction, cytokinin signaling, and vascular tissue patterning (Fig. 5B) [57–60]. Among those potential gene programs, several differentially expressed genes pairs were affected by HE. Those genes include *FLC.A03-C03* and *FLC.A10-C09* for the late-flowering signal transduction, *TMO6.A03-C03* for cytokinin signaling and *XCP1.A01-C01* gene pairs for vascular tissue differentiation and development (Fig. 5C; Additional file 1: Fig. S28). These findings suggest that HEs influence these biological processes, potentially involving the morphological changes in swede.

Selections of HEs in domesticated *Brassica* juncea crops

To test whether selective significance of HEs on trait domestication as revealed in *B. napus* is a generic property of allopolyploids, we analyzed another *Brassica* allopolyploid species, *B. juncea* (AABB genome), with publicly available genome sequence data [61]. We characterized the HE events in the domestication of *B. juncea* species, including 425 accessions across six populations, and compared the results with those of *B. napus*. A set of 28,934 homologous gene pairs were identified by applying the same method to determine the collinearity between the A and B subgenomes, which revealed much lower collinearity of the two subgenomes in *B. juncea* compared to *B. napus* (Additional file 1: Fig. S29). HEs were also detected in *B. juncea* accessions; however, the extent of HEs was much lower than in *B. napus* (Fig. 6). In particular, we identified two large HE segments of A replacing B in the root mustard morphotype (G1_Root) on chromosome B01, which were replaced by the corresponding homoeologous A04 and A05 segments, respectively (Additional file 1: Fig. S30). Although HE segments in A04 and A05 were also found in swede (*B. napus*), the specific position of these segments did not match with those found in root mustard (*B. juncea)*. Those group-level HE segments may indicate potential selection of additional independent HE patterns to the tuber-forming morphotype in *B. juncea* (Additional file 2: Table S13). Those HE regions also contained several genes related to tuber development, such as *STP6.A05-B01* (*SUGAR TRANSPORTER 6*), *EXPA4.A04-B01* (*EXPANSION A4*), among others (Additional file 2: Table S14). In general, the occurrence of HEs at group level indicates their likely evolutionary significance in polyploid species, contributing to adaptation and domestication for favorable traits.

Discussion

Homoeologous exchanges have been commonly observed in both newly synthesized and established allopolyploid crop species, suggesting their potential role in species diversification and crop domestication. However, their specific contributions to the domestication of allopolyploid crops and their impact on trait diversification have yet to be thoroughly researched. In this study, we conducted a comprehensive analysis of HEs in the domestication of polyploid *Brassica* species. By exploring the genomic patterns of HEs across diverse morphotypes and individuals, we connected HEs to phenotypic

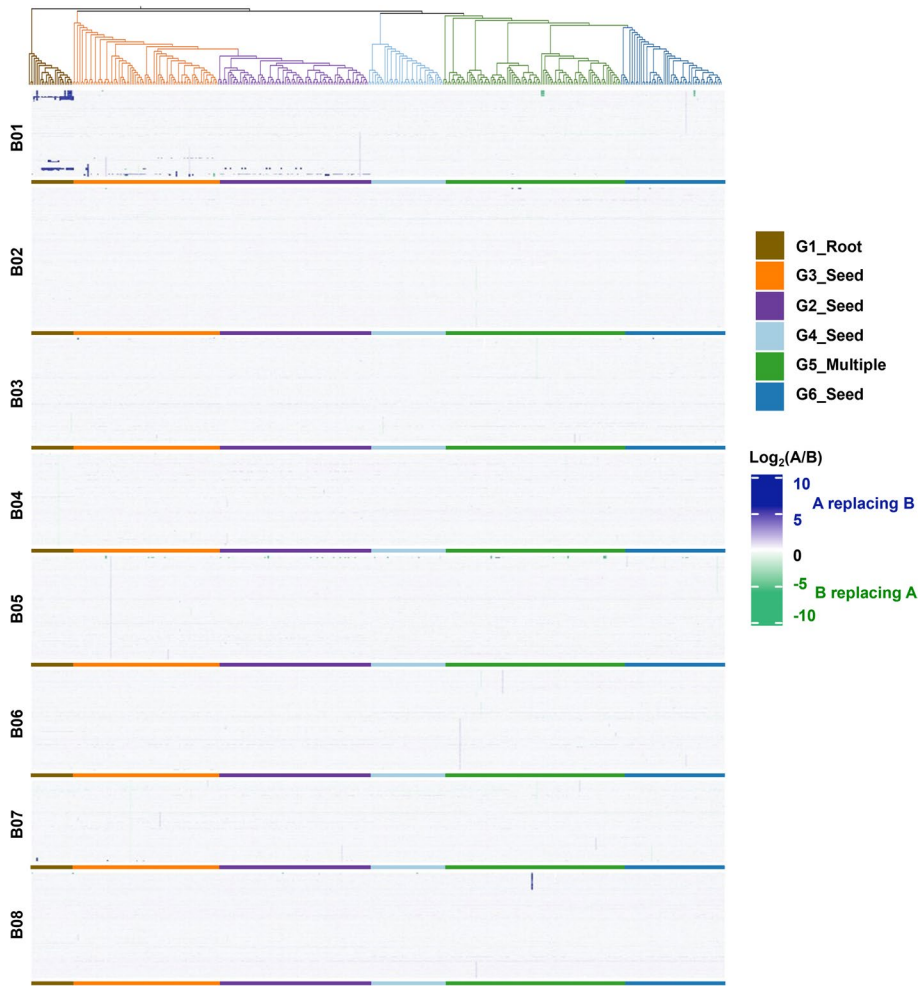

Fig. 6 The occurrence of homoeologous exchanges between A and B genome during the domestication of *Brassica juncea*, as indicated by B genome coordinate. Four hundred twenty five accessions of *B. juncea* are ordered based on phylogenetic relationship, sourced from Kang et al. [61]. Name of each group is defined based on research. Group names are indicated as the colored bars at the bottom. The homoeologous exchange values represent $\log_2$-transformed mapping density ratios of the homoeologous gene pairs, with the blue and purple components representing the coverage abundance of the A and B genome, respectively. The homoeologous gene pairs are plotted on the Y axis as B genome chromosomes ordered from B01 to B08 and on the X axis based on the phylogenetic relationships of all accessions. Homoeologous relationship between A and B genome can be found in Supplementary Figure S29

changes. Taken together, our findings highlight the importance of HE for allopolyploid crop domestication.

The role of HEs during the polyploid genome evolution

For newly formed tetraploids, polyploidization seems to be a coin with two sides. Although polyploidy greatly expands genome instability and genomic shocks with direct implications for short-term survival, it can open up access to genetic novelties on which natural and human selection can act [9, 16]. Following polyploidization, homoeologous exchange events have been shown to induce significant variations in both the genomic and transcriptomic landscapes, thus leading to the emergence of adaptive

traits. Our findings reveal an extensive prevalence of HEs in *B. napus* and certain HEs have been selected during the domestication of morphotypes in allopolyploid *Brassica* species (Figs. 1 and 6). Intriguingly, certain HEs are exclusive to specific accessions and are absent in phylogenetically related ones, indicating that they have arisen and been selected during the recent breeding and domestication of this germplasm. This finding supports the notion that HEs are actively participating in generating variations contributing to the recent domestication processes [42]. Other HEs are shared among accessions or across morphotypes, suggesting that the potential ancestral state of these signals was selected during intraspecies diversification [62]. In fact, those HE-affected accessions represent "segmental autopolyploid in allopolyploids", which contain a mixture of partial autopolyploid segments within an allopolyploid genome [17]. In this study, through the de novo assembly of a swede reference genome, we have confirmed the HE signals in this reference genome that were initially identified by the short-read data (Fig. 5B). The newly assembled reference genome of the segmental allopolyploid swede highlights the complexity of its genome structure, as it comprises a complex mosaic of genomic regions representing one or the other subgenome, with considerable relevance for phylogenomics [37].

Mechanisms and patterns of HEs in allopolyploid genomes

Understanding the mechanisms leading to HEs in allopolyploid genome should be traced back to the meiotic pairing process, as the inherited homoeologous chromosomes from progenitors still have the potential to pair with each other [31, 32]. Aside from genes related to pairing control mechanisms as depicted previously [36, 63], features intrinsic to the allopolyploid genome and differences in intrinsic homoeologous genome divergence also have an impact on the occurrence of HEs [64]. In our study, we found the genomic regions where exchanges have taken place are not random. Instead, HEs tend to occur in the distal regions of chromosome arms of high gene density and high recombination frequency. This spatial pattern suggests a strong association between HEs and these specific chromosomal regions (Fig. 2A). The prevalence of HEs extending towards telomeres supports the notion that sub-telomeric regions play a role in homoeologous recognition and selection [29, 65]. Additionally, our study highlights a subgenome bias in the directional replacement of HEs within allopolyploid *Brassica* species. The A genome from *B. rapa* exhibits a higher propensity to replace segments of the B and C genomes (*B. nigra*, *B. oleracea*), indicating its genome dominance in HE events (Figs. 2B, C and 6). Similar pattern of biased HEs towards one subgenome has also been found in other allopolyploid species including peanut [30] and strawberry [66], suggesting HEs as a potential cause for subgenome dominance [37].

Furthermore, sequence homology can explain the occurrence of HEs in allopolyploids. HEs were found to be significantly different in AACC genome compared with AABB genome (Figs. 1 and 6). Such different frequency of HEs can be mainly attributed to the differences in sequence homology, which can be explained in two aspects. Firstly, the collinearity between the A and B ancestral genomes is much lower than that of the A and C genome. The reduced collinearity in the A and B genome in *B. juncea* indicates a lower possibility of pairing during the meiosis phase (Figs. S3, S29). Previous research on synthetic allopolyploid rice (*Oriza sativa*), which was generated by hybridization and

doubling of two highly syntenic parental rice subspecies (*japonica* and *indica*), revealed extremely frequent HE events among its descendants, with some individuals even exhibiting complete replacement of whole chromosomes with those from the other subspecies [24]. Secondly, the lower frequency of HEs in AABB genomes may also be due to the decreased sequence similarity of collinear genes or collinear regions. The divergent time between the A and C genome occurred approximately 4.6 million years ago (Mya), while the divergence between the A and B genome happened around 6.5 Mya [67]. The significantly longer divergence time of the A and B genomes suggests a greater degree of sequence divergence in their collinear regions. This divergence could also affect the homoeologous chromosome pairing efficiency, which drives the occurrence of HEs in allopolyploids.

Importance of HE compared with other genetic variations

The evolution and domestication of species involve a complex interplay of genetic changes that shape their genomes and phenotypes. Among these genetic variations, homoeologous exchanges stand out as a unique and potent mechanism in allopolyploid species evolution. In comparison to other genetic variations like point mutations, small-scale structural changes, and chromosomal rearrangements, HEs offer distinct advantages that contribute significantly to genome evolution and phenotypic diversity [19]. One key distinction of HE lies in their large-scale impact, where HEs facilitate the replacement of substantial chromosome segments between homoeologous chromosomes that include not only genes but also their associated regulatory elements [23]. In our study, certain *B. napus* accessions exhibited the replacement of C genome segments spanning up to 12.6 Mb with their A genome counterparts (Fig. 1). Notably, these large-scale replacements can extend to entire chromosomes, as observed in resynthesized allopolyploid rice [24]. This ability to induce large structural changes is especially critical for driving rapid and substantial shifts in phenotypes. Furthermore, the direct and immediate connection between HEs and phenotypic changes makes them indispensable contributors to trait diversification [68]. Their persistence across both newly synthesized allopolyploids and established species underscores their evolutionary significance (Figs. 1 and 6). The recurring, selection-driven occurrence of HEs emphasizes their active role in species diversification and crop domestication.

Selection of HEs in *Brassica* morphotypes domestication

The allopolyploid species in the *Brassica* genus contain various morphotypes and ecotypes, which have been distributed and domesticated worldwide in various habitats. Yet, they are relatively new species, with a hybridization history of around 10,000 years and a severe bottleneck of population size following their speciation [48, 61]. Understanding how allopolyploid *Brassica* crops have, despite this severe genomic bottleneck, adapted to different environments globally is crucial for a full appreciation of their domestication and utilization. In our previous study, we emphasized the role of interploidy introgression from diploid *Brassica* crops in the adaptation of the polyploid *B. napus* [48]. In this study, we focus on another important mechanism of polyploidization, HEs, in the diversification and domestication of various morphotypes and ecotypes in *B. napus* and *B. juncea*. Research has suggested the

potential contributions of HEs to various traits in *Brassica* species, including seed oil content and disease resistance, which are crucial for agricultural success and adaptability [29, 38]. However, these studies often focused on the immediate genetic outcomes of HEs, especially in those synthetic plants, often overlooking their broader implications on the domestication narrative. Our study bridges this gap by illustrating that HEs are not only actively occurring in polyploid *Brassica* crops but also under selective forces during domestication. For instance, our observations of distinct HE patterns in swede and Siberian kale morphotypes suggest an adaptive advantage conferred by specific HE events in response to environmental and agricultural selection (Fig. 3). Specifically, the swede morphotype had the most notable HE patterns, involving many functional important homoeologous gene pairs associated with flowering time diversification and hypocotyl root development (Figs. 4 and 5). Other groups from *B. napus* and *B. juncea* have a moderate level of HE signals, with taxon-specific patterns present in all three ecotypes, containing many genes potentially affecting their phenotypes. Those group-level HE patterns are common among the various morphotypes and ecotypes, indicating their selective role in the domestication process for crops.

Mechanisms contributing to tuberous organ formation in allopolyploid *Brassica*

The Brassica genus exhibits a remarkable divergence in morphotypes, alongside instances of convergent evolution across different species. Notably, tuberous organs such as the swollen hypocotyl-root vegetables found in turnip (*B. rapa*, AA), swede (*B. napus*, AACC), and root mustard (*B. juncea*, AABB) represent some of the earliest morphotypes to emerge during their independent domestication processes [48, 61]. This suggests an ancient preference for these morphotypes, likely due to their starch and sugar content, which are significant components in early human diets. In allopolyploid species, the emergence of tuberous organs as initial domesticated morphotypes underscores the role of polyploidization and convergent evolution in shaping crop characteristics. In our study, we found that HEs may contribute to the tuberous organ during the domestication of *B. napus* and *B. juncea*. Among the different morphotypes in *B. napus*, swede exhibited the highest incidences of HE events compared to other morphotypes, indicating the potential importance of HEs selection for the swede domestication (Fig. 3). By comparing the expression levels of genes during the initiation and development of swede tubers, many of the HE-affected genes were found to be differentially expressed, suggesting that HE-induced changes may play some role in swede hypocotyl-root tuber development (Fig. 5). In *B. juncea*, root mustard was the main morphotype with two large HE segments of A replacing B on chromosome B01, indicating the potential selection of HEs for this morphotype (Fig. 6). The specific A genome position of HEs segments in root mustard did not match with those found in swede, but those HE regions also contained several genes related to tuber development. Tuberous organ formation is a complex trait which has hardly been studied in *Brassica* species. We speculate that various genome evolution processes contributed to the tuber trait formation during domestication, including interploidy introgression, homoeologous exchanges, and independent

and convergent genomic selection from the genomes (A, B, C) resulting from recent polyploidy and paleo-subgenomes (LF, MF1 and MF2) from ancient polyploidy.

Conclusions

In this study, we conducted a detailed analysis of homoeologous exchanges in the domestication of two polyploid *Brassica* species. Our exploration of genomic patterns of HEs across various morphotypes and accessions established a direct link between HEs and phenotypic variations. We identified specific HE patterns that contribute to the flowering-time diversification in different ecotypes and development of hypocotyl-root in swede. This investigation highlights the significance of HEs in polyploid crops genomic diversity and adaptability, revealing their contribution to the domestication processes. In conclusion, HE represents a major mechanism to induce phenotypic innovation in allopolyploid plants via generating novel genomic composition and inducing transcriptional variation. The continuous studies for homoeologous exchanges and its mechanisms could ultimately offer new breakthrough for us to improve diversities in polyploid crops.

Methods

Plant materials and data collection

The diversity panel of *Brassica napus* used in this study comprised 260 accessions, including 55 accessions of swede/rutabaga (*B. napus* subsp. *rapifera*), 21 accessions of Siberian kale (*B. napus* subsp. *pabularia*), and 184 accessions of rapeseed (*B. napus* subsp. *oleifera*). Besides, we also collected 8 accessions of presumed diploid progenitors of European turnip (*B. rapa* subsp. *rapa*) and wild type of *B. oleracea* (*B. oleracea* subsp. *acephala*). One swede accession named "Laurentian" (Bna007) was used for genome assembly in this study. Seeds were planted in the greenhouse during autumn 2020 in order to confirm morphotypes. Fresh leaves were collected for DNA extraction and library preparation. Detailed information about resources, morphotypes, and ecotypes for each accession is shown in supplementary table S1.

Genome resequencing reads alignment and variants calling

Given that using the *B. napus* AC reference genomes for HE analysis could introduce biases due to its potential pre-existing HEs, we select the reference genome of the diploid ancestral species *B. rapa* [69] (AA, Chiifu version 3), and *B. oleracea* [70] (CC, JZC version 2). The two diploid genomes were concatenated to represent the genome of *B. napus*. The raw reads data from all accessions were filtered to remove low-quality bases using fastp (version 0.23), with parameters "-q 20 -u 30 -n 6 -c" [71]. The filtered sequencing reads of *B. napus* were aligned to the combined genome with BWA-MEM (version 0.7.12) employing default parameters, followed by sorting of alignment results, and marking of PCR duplicates with Sambamba (version 0.7) [72]. The mapping quality of each accession were checked for their alignment statistics using Qualimap2 [73] (Table S1). Variants calling for each accession was performed using GATK HaplotypeCaller module in accordance with Genome Analysis

Toolkit (GATK) Best Practices [74] and merged into a single GVCF file model, from which SNPs were subsequently identified using a joint calling approach.

Inference of phylogenetic relationship

To understand the phylogenetic relationships in the domestication history of *B. napus*, a maximum-likelihood phylogenetic tree was constructed using fourfold degenerate sites SNPs in order to reduce the potential influence of selection bias. Phylogenetic tree was built using IQ-TREE (version 2.0.3) [75], based on the best fitting model (TVM + R10), determined by the Bayesian information criterion. Bootstrap values were calculated for 1000 iterations using the ultrafast bootstrap method (UFboot). The output file was then plotted with the 8 ancestral accessions as the outgroup, and visualized with the R package ggtree [76].

Detection of homoeologous exchanges

Assessment of read coverage depth was used to detect homoeologous exchange patterns between the A and C subgenomes; homoeologous gene pairs were used as anchors to assess the patterns (Additional file 1: Fig. S2) (adapted and revised from He et al. [29]). We focused on non-reciprocal exchanges as reciprocal exchanges are less frequently observed and pose greater challenges for detection using sequencing-based methods. A total of 31,456 syntenic homoeologous gene pairs between the A and C genome were identified using SynOrth, based on both the sequence similarity and homologous flanking genes [77]. To identify HE, an mpileup file for each accession was generated using samtools from the BAM file [78], which was subsequently processed to obtain mapping depth for each of the defined homoeologous gene anchored on chromosomes (Fig. S4). We also utilized in silico ancestral accessions of *B. napus*, generated by 64 pairwise combinations of sequencing data from 8 European turnip of *B. rapa* and 8 wild type of *B. oleracea*. These in silico accessions represent genetic and technical background for *B. napus* prior to any HEs, thereby providing a control group for comparison of HE signals in the real *B. napus* accessions.

HE ratios were calculated by dividing the mapping depth of the A gene by that of the corresponding C gene and were subsequently $\log_2$-transformed ($\log_2$(A/C)). Deviations from zero in the log2-transformed values indicate a potential occurrence of homoeologous exchange between gene pairs, with values greater than threshold of 2 indicating A replacing C and values less than −2 indicating C replacing A. In contrast, clustering of $\log_2$-transformed values around zero reveals unaltered homoeologous gene pairs that have not undergone HE. In addition, to mitigate potential bias caused by local gene duplication/gene loss, HE values deviating from zero were cross-verified against the mapping densities of both homoeologous genes. An HE value was maintained if the mapping depth of one homoeologous gene exceeded 1.5 times the overall read depth in the accession, and simultaneously the other gene was less than 0.375 times. Otherwise, the HE value was reset to zero (Additional file 1: Fig. S5). These $\log_2$-transformed HE value was then visualized according to their order on chromosome number and position at the basis of the C genome by customized scripts in R. HE regions were defined based on the mean value of sliding window of

5 genes with step of 2 genes across the genome. Those windows were further filtered and merged based on the threshold absolute value of 2.

Identification of group-level homoeologous exchange

Group-level homoeologous exchange (HE) patterns were investigated across different morphotypes and ecotypes of *B. napus*, including swede, Siberian kale, winter rapeseed, spring rapeseed, and semi-winter rapeseed. The group-level HE for different morphotypes was calculated as the average value of HE ratio for all the accessions in this group using a sliding window of 5 genes with steps of 2 genes across the genome. Mann–Whitney test was performed to assess the significance of differences in HE values between various groups and the in silico control in *B. napus*. For HE values showing deviation from zero, only those that showed significant differences compared to the control group were retained ($P < 0.01$). Windows with absolute HE values exceeding 2 were subsequently merged to represent the group-level HE regions.

De novo assembly of a swede genome and gene annotation

Genomic DNA was isolated from young leaves using a cetyltrimethylammonium bromide (CTAB) method. Both Illumina short-read library and ONT long-read sequencing library were prepared according to standard manufacturer's protocol. The resulting dataset consisted of approximately 110 Gb of Illumina reads and 97 Gb of Nanopore reads for de novo assembly of the swede genome. The BL-Hi-C libraries were constructed following a previous protocol and processed into paired-end sequencing libraries, resulting in ~ 105 Gb paired-end Hi-C reads for genome scaffolding [79].

The raw ONT long reads were self-corrected using the NextCorrect module in NextDenovo [80]. The corrected reads were assembled into contigs using the Canu assembler (version 2.2) [81], with optimized parameters 'batOptions = -dg 3 -db 3 -dr 1 -ca 500 -cp 50'. Contigs were polished using both the corrected ONT reads and highly accurate short reads with NextPolish [82]. Chromosome-level genome assemblies were obtained using Hi-C. The Hi-C mapping results were processed to obtain the contact signals using the 3D-DNA pipeline [83]. The resulting assembly was further corrected using the visualization of chromatin contact patterns with the Juicebox Assembly Tools, leading to 19 pseudochromosomes [84].

The gene structure was annotated using the MAKER2 pipeline [85], integrating evidence from transcriptomes, protein homologs, and ab initio methods for gene structure prediction. EVM was used to integrate all predicted gene structure evidence, producing high-confidence gene models [86]. Gene functions were assigned based on alignments with the eggNOG v5.0 database using the eggNOG-mapper with default settings [87, 88]. Genome quality was evaluated using the BUSCO pipeline [89] to assess the completeness of the gene space.

Confirmation of HE by whole genome comparison

Syntenic regions between the two diploid genomes of *B. rapa* and *B. oleracea* were identified using MCScan with parameters "-a -e 1e-5 -s 5" [90]. Syntenic blocks comprising of at least 5 genes were obtained and further visualized using graphic module implemented in jcvi [91]. The swede assembled genome was also compared to their diploid

progenitors of *B. rapa* and *B. oleracea* using Mummer based on the minimum clustering unit of 10 Kb with parameters (nucmer –maxmatch -l 80 -c 200). The output was further visualized with dotPlotly [92].

Expression analysis for HE-related genes

For exploring the effect of HEs on gene expression changes in different morphotypes of *B. napus*, we selected the accessions which have both public resequencing data and public transcriptome data available [46]. According to previous description, both RNA and DNA were collected from the second youngest leaf of the accession when the plant had five true leaves. All raw paired-end RNA-seq reads were filtered with fastp and further mapped to the concatenated reference genomes of *B. rapa* (AA), and *B. oleracea* (CC) using STAR (version 2.7.10) [93]. RSEM was used to estimate the expression levels, which utilized expectation maximization (EM) algorithm to estimate the maximum likelihood value of gene or transcript abundance after taking multi-mapped reads into account [94]. Gene expression level was calculated based on the transcripts per million reads (TPM) values. To assess HE's impact on overall gene expression, genes within the HE regions in each accession were designated as HE-related genes and the rest as non-HE genes. The average expressional value of HE-related genes in HE-harboring accessions was compared with those in HE-free accessions. For expressional changes of total homoeologous gene pair, we first compare the expression between A and C genes in those non-HE accessions, and identify those differentially expressed gene of either higher expression of A or C. For those differentially expressed genes in non-HE accessions, those genes were assigned as the pre-HE status. Second, for those differentially expressed genes, we further investigate the effects of HEs on overall expression of gene pair. The results were further visualized using R ggplot2.

Transcriptome analysis for root tuberization

In order to explore potential effect of HEs on the tuberization process, the tuber-forming swede accession and a rapeseed accession was cultivated for their hypocotyl root tissues during the tuberization process. Both hypocotyl root tissues were collected for swede and rapeseed at three timepoints around tuber initiation stage (21, 28, 35 days after sowing) with three replicates. The total RNA for each accession at each timepoint was isolated and sequenced according to the standard protocols. Gene expression analysis was performed as described before. Differentially expressed genes between swede and rapeseed at each timepoint were identified using DESeq2 [95]. Enrichment analysis of HE genes among differentially expressed genes was tested by Fisher's exact test (differentially expressed gene pair ratio: 865 HE/4347 total, background ratio: 1405 HE affected/31,456 syntenic homoeologous gene pairs). Expression changes of the representative HE-related genes were further compared and visualized in R.

Identification of homoeologous exchanges in *B. juncea*

We analyzed an additional *Brassica* allopolyploid species, *B. juncea*, with publicly available genome sequence data to test the selective significance of HEs in

domestication [61]. The diversity panel of *Brassica juncea* used in this study comprised 425 accessions from 6 groups classified previously. All public re-sequencing data used in this study were downloaded from National Center for Biotechnology Information (NCBI) Sequence Read Archive collection (SRA). The reference genome of diploid ancestral species *B. rapa* (AA, Chiifu version 3), and *B. nigra* [96] (BB, Ni100) were concatenated to represent the AABB genome of *Brassica juncea*. Twenty eight thousand nine hundred thirty four homoeologous gene pairs between the AA and BB genome were identified through reciprocal best match. Identification of HE for 425 accessions and 6 groups were performed as described before.

Supplementary Information

The online version contains supplementary material available at https://doi.org/10.1186/s13059-024-03370-z.

Additional file 1: Figure S1. Phylogenetic tree of *B. napus*. Figure S2. Workflow for identification of homoeologous exchange. Figure S3. Homoeologous relationships between *Brassica* A and C genomes. Figure S4. Example of Homoeologous exchanges detected by the raw reads mapping depth across homoeologous chromosomes A01-C01 in Bna006 accession. Figure S5. Distribution of relative mapping depth between homoeologous A and C gene pairs. Figure S6. Illustration of homoeologous exchanges signals for 64 in silico *B. napus* accessions. Figure S7. Illustration of HE signals for eight rapeseed accessions with the assembled genomes. Figure S8-S16. The occurrence of homoeologous exchange between each of the A and C genome in *B. napus*, as indicated by the C genome coordinate. Figure S17. The occurrence of HEs in 119 public accessions of *Brassica napus*. Figure S18. Effects of HEs on gene expressional alternations in 119 accessions of *Brassica napus*. Figure S19. Proposed model describing selection and fixation of HE patterns in populations. Figure S20. Upset plot comparison showing the numbers of HE gene pairs in different groups for "A replacing C" and "C replacing A" events, respectively. Figure S21. Upset plot comparison of groups showing the numbers of flowering-time related gene pairs affected by HE. Figure S22. Impact of homoeologous exchanges on three *FLC* gene pairs in different groups. Figure S23. Impact of homoeologous exchanges on three *FLC* gene pairs and their expressional changes. Figure S24. Expression levels of *BnaFLC.A10* and two *BnaFLC.C09* genes in young leaves. Figure S25. The Hi-C intra-chromosomal heatmap. Figure S26. Homoeologous exchanges between A and C genome in swede genome measured by both short-reads and long-reads data. Figure S27. Whole genome comparison between the swede genome and concatenated genome of *B. rapa* and *B. oleracea*. Figure S28. Differential expression of HE-affecting gene pairs in root development of swede and rapeseed. Figure S29. Homoeologous relationships between *Brassica juncea* A and B genome. Figure S30. The occurrence of homoeologous exchanges during the domestication of *Brassica juncea*, as indicated by A genome coordinate.

Additional file 2: Table S1. Detailed information of *Brassica* accessions in this study. Table S2. Homoeologous gene pairs between A and C genome. Table S3. Homoeologous exchange regions in *B. napus* accessions based on C genome coordinate. Table S4. Group-level homoeologous exchange value among the five morpho/ecotypes of *B. napus*. Table S5. List of homoeologous gene pairs associated with the flowering process. Table S6. List of flowering related homoeologous gene pairs affected by HE events in each morphotypes. Table S7. Flowering time record of 123 accessions used in this study. Table S8. Sequencing data used for the swede genome assembly. Table S9. Statistics of assemblies and annotation in Swede genome. Table S10. Statistics of the annotated genes for the swede assembly. Table S11. BUSCO comparison of different genome assembly in *B. napus*. Table S12. Average expression profile of homoeologous gene pairs in hypocotyl-root development. Table S13. Group-level homoeologous exchange value among the 6 groups of *B. juncea*. Table S14. Genes affected by homoeologous exchange among the 6 groups of *B. juncea*.

Additional file 3. Review history.

Acknowledgements
We thank Prof. Jian Wu, Dr. Jianli Liang, Dr. Xu Cai, Dr. Hongbo Li, Celia Anton Sales, and Wei Sun for their comments and discussion of the research. We thank Rogier Weel and Zihan Liu for the help in analyzing cytological photos. We acknowledge Wageningen University Unifarm greenhouse for their help with the maintenance of the plants.

Peer review information
Qingxin Song and Wenjing She were the primary editors of this article and managed its editorial process and peer review in collaboration with the rest of the editorial team.

Review history
The review history is available as Additional file 3.

Authors' contributions
T.W. analyzed and interpreted the data, drafted and revised the manuscript. T.W. and R.Z. grew plants, collected tissues, and performed experiments. A-J.D., G.B., and X.W. conceived the research, supervised the experiment and data analysis, and modified the manuscript. All authors read and approved the final manuscript.

Funding
This work was supported by the National Key Research and Development Program of China (2021YFF1000104), the Agricultural Science and Technology Innovation Program (ASTIP), Beijing Municipal Science and Technology Project (Z231100003723009), the Central Public-interest Scientific Institution Basal Research Fund (Y2023PT16), and TKI project (KV1605-004). T.W. acknowledges the China Scholarship Council (No. 202003250137), the NPO bursary funding from Wageningen university, and the scholarship from Institute of vegetables and flowers.

Availability of data and materials
Previously published whole-genome resequencing data of ***Brassica*** accessions, listed in Additional file 2: Table S1, were downloaded from the NCBI database under the accession number PRJNA888419 [48], PRJNA428769 [46], and PRJNA476657 [54]. The genome and transcriptome raw data of the samples produced in this study have been deposited in the Sequence Read Archive (SRA) under the BioProject accession number PRJNA1050615 [97]. The swede genome assembly and gene annotation are available from the Genome warehouse database of the National Genomics Data Center under accession number PRJCA028594 [98]. The scripts associated with this project were deposited at the GitHub [99] and Zenodo [100]. The genome assembly and codes are also available via the BRAD website (http://brassicadb.cn/) [101].

Declarations

Ethics approval and consent to participate
Not applicable.

Competing interests
The authors declare that they have no competing interests.

Received: 10 December 2023 Accepted: 10 August 2024
Published online: 27 August 2024

References

1. Van de Peer Y, Mizrachi E, Marchal K. The evolutionary significance of polyploidy. Nat Rev Genet. 2017;18:411–24.
2. Soltis DE, Albert VA, Leebens-Mack J, Bell CD, Paterson AH, Zheng C, Sankoff D, Depamphilis CW, Wall PK, Soltis PS. Polyploidy and angiosperm diversification. Am J Bot. 2009;96:336–48.
3. Stebbins GL. Chromosomal evolution in higher plants. London: Edward Arnold Ltd.; 1971.
4. Van de Peer Y, Ashman T-L, Soltis PS, Soltis DE. Polyploidy: an evolutionary and ecological force in stressful times. Plant Cell. 2020;33:11–26.
5. Jiao Y, Leebens-Mack J, Ayyampalayam S, Bowers JE, McKain MR, McNeal J, Rolf M, Ruzicka DR, Wafula E, Wickett NJ, et al. A genome triplication associated with early diversification of the core eudicots. Genome Biol. 2012;13:R3.
6. Leebens-Mack JH, Barker MS, Carpenter EJ, Deyholos MK, Gitzendanner MA, Graham SW, Grosse I, Li Z, Melkonian M, Mirarab S, et al. One thousand plant transcriptomes and the phylogenomics of green plants. Nature. 2019;574:679–85.
7. Landis JB, Soltis DE, Li Z, Marx HE, Barker MS, Tank DC, Soltis PS. Impact of whole-genome duplication events on diversification rates in angiosperms. Am J Bot. 2018;105:348–63.
8. Udall JA, Wendel JF. Polyploidy and crop improvement. Crop Sci. 2006;46:S–3.
9. Renny-Byfield S, Wendel JF. Doubling down on genomes: polyploidy and crop plants. Am J Bot. 2014;101:1711–25.
10. Salman-Minkov A, Sabath N, Mayrose I. Whole-genome duplication as a key factor in crop domestication. Nat Plants. 2016;2:16115.
11. Hilu KW. Polyploidy and the evolution of domesticated plants. Am J Bot. 1993;80:1494–9.
12. Arrigo N, Barker MS. Rarely successful polyploids and their legacy in plant genomes. Curr Opin Plant Biol. 2012;15:140–6.
13. Nieto Feliner G, Casacuberta J, Wendel JF. Genomics of evolutionary novelty in hybrids and polyploids. Front Genet. 2020;11:792.
14. Soltis DE, Visger CJ, Soltis PS. The polyploidy revolution then...and now: Stebbins revisited. Am J Bot. 2014;101:1057–78.
15. Schiessl S-V, Katche E, Ihien E, Chawla HS, Mason AS. The role of genomic structural variation in the genetic improvement of polyploid crops. Crop J. 2019;7:127–40.
16. Baduel P, Bray S, Vallejo-Marin M, Kolář F, Yant L. The "Polyploid Hop": shifting challenges and opportunities over the evolutionary lifespan of genome duplications. Front Ecol Evol. 2018;6:117.
17. Mason AS, Wendel JF. Homoeologous exchanges, segmental allopolyploidy, and polyploid genome evolution. Front Genet. 2020;11:1014.
18. Alger EI, Edger PP. One subgenome to rule them all: underlying mechanisms of subgenome dominance. Curr Opin Plant Biol. 2020;54:108–13.
19. Deb SK, Edger PP, Pires JC, McKain MR. Patterns, mechanisms, and consequences of homoeologous exchange in allopolyploid angiosperms: a genomic and epigenomic perspective. New Phytol. 2023;238:2284–304.
20. Glover NM, Redestig H, Dessimoz C. Homoeologs: what are they and how do we infer them? Trends Plant Sci. 2016;21:609–21.
21. Gaeta RT, Pires JC. Homoeologous recombination in allopolyploids: the polyploid ratchet. New Phytol. 2010;186:18–28.

22. Yim WC, Swain ML, Ma D, An H, Bird KA, Curdie DD, Wang S, Ham HD, Luzuriaga-Neira A, Kirkwood JS, et al. The final piece of the Triangle of U: evolution of the tetraploid Brassica carinata genome. Plant Cell. 2022;34:4143–72.
23. Zhang Z, Gou X, Xun H, Bian Y, Ma X, Li J, Li N, Gong L, Feldman M, Liu B, Levy AA. Homoeologous exchanges occur through intragenic recombination generating novel transcripts and proteins in wheat and other polyploids. Proc Natl Acad Sci U S A. 2020;117:14561–71.
24. Wu Y, Lin F, Zhou Y, Wang J, Sun S, Wang B, Zhang Z, Li G, Lin X, Wang X, et al. Genomic mosaicism due to homoeologous exchange generates extensive phenotypic diversity in nascent allopolyploids. Nat Sci Rev. 2020;8(5):nwaa277
25. Yu H, Lin T, Meng X, Du H, Zhang J, Liu G, Chen M, Jing Y, Kou L, Li X, et al. A route to de novo domestication of wild allotetraploid rice. Cell. 2021;184(5):1156–1170.e14.
26. Osborn TC, Butrulle DV, Sharpe AG, Pickering KJ, Parkin IAP, Parker JS, Lydiate DJ. Detection and effects of a homeologous reciprocal transposition in Brassica napus. Genetics. 2003;165:1569–77.
27. Gaeta RT, Pires JC, Iniguez-Luy F, Leon E, Osborn TC. Genomic changes in resynthesized Brassica napus and their effect on gene expression and phenotype. Plant Cell. 2007;19:3403–17.
28. Chalhoub B, Denoeud F, Liu S, Parkin IA, Tang H, Wang X, Chiquet J, Belcram H, Tong C, Samans B, et al. Early allopolyploid evolution in the post-Neolithic *Brassica napus* oilseed genome. Science. 2014;345:950–3.
29. He Z, Wang L, Harper AL, Havlickova L, Pradhan AK, Parkin IAP, Bancroft I. Extensive homoeologous genome exchanges in allopolyploid crops revealed by mRNAseq-based visualization. Plant Biotechnol J. 2017;15:594–604.
30. Bertioli DJ, Jenkins J, Clevenger J, Dudchenko O, Gao D, Seijo G, Leal-Bertioli SCM, Ren L, Farmer AD, Pandey MK, et al. The genome sequence of segmental allotetraploid peanut Arachis hypogaea. Nat Genet. 2019;51:877–84.
31. Pelé A, Rousseau-Gueutin M, Chèvre A-M. Speciation success of polyploid plants closely relates to the regulation of meiotic recombination. Front Plant Sci. 2018;9:907.
32. Mercier R, Mezard C, Jenczewski E, Macaisne N, Grelon M. The molecular biology of meiosis in plants. Annu Rev Plant Biol. 2015;66:297–327.
33. Lloyd A, Bomblies K. Meiosis in autopolyploid and allopolyploid Arabidopsis. Curr Opin Plant Biol. 2016;30:116–22.
34. Griffiths S, Sharp R, Foote TN, Bertin I, Wanous M, Reader S, Colas I, Moore G. Molecular characterization of Ph1 as a major chromosome pairing locus in polyploid wheat. Nature. 2006;439:749–52.
35. Jenczewski E, Eber F, Grimaud A, Huet S, Lucas MO, Monod H, Chèvre AM. PrBn, a major gene controlling homeologous pairing in oilseed rape (Brassica napus) haploids. Genetics. 2003;164:645–53.
36. Higgins EE, Howell EC, Armstrong SJ, Parkin IAP. A major quantitative trait locus on chromosome A9, BnaPh1, controls homoeologous recombination in Brassica napus. New Phytol. 2021;229:3281–93.
37. Edger PP, McKain MR, Bird KA, VanBuren R. Subgenome assignment in allopolyploids: challenges and future directions. Curr Opin Plant Biol. 2018;42:76–80.
38. Hurgobin B, Golicz AA, Bayer PE, Chan CK, Tirnaz S, Dolatabadian A, Schiessl SV, Samans B, Montenegro JD, Parkin IAP, et al. Homoeologous exchange is a major cause of gene presence/absence variation in the amphidiploid Brassica napus. Plant Biotechnol J. 2018;16:1265–74.
39. Lloyd A, Blary A, Charif D, Charpentier C, Tran J, Balzergue S, Delannoy E, Rigaill G, Jenczewski E. Homoeologous exchanges cause extensive dosage-dependent gene expression changes in an allopolyploid crop. New Phytol. 2018;217:367–77.
40. Zhang Z, Xun H, Lv R, Gou X, Ma X, Li J, Zhao J, Li N, Gong L, Liu B. Effects of homoeologous exchange on gene expression and alternative splicing in a newly formed allotetraploid wheat. Plant J. 2022;111(5):1267–82.
41. Pires JC, Zhao J, Schranz ME, Leon EJ, Quijada PA, Lukens LN, Osborn TC. Flowering time divergence and genomic rearrangements in resynthesized Brassica polyploids (Brassicaceae). Biol J Lin Soc. 2004;82:675–88.
42. Schiessl S, Huettel B, Kuehn D, Reinhardt R, Snowdon R. Post-polyploidisation morphotype diversification associates with gene copy number variation. Sci Rep. 2017;7:41845.
43. Heslop-Harrison P. Genetics, genomics and breeding of oilseed brassicas. Ann Bot. 2013;112:vi–vi.
44. Song J-M, Guan Z, Hu J, Guo C, Yang Z, Wang S, Liu D, Wang B, Lu S, Zhou R, et al. Eight high-quality genomes reveal pan-genome architecture and ecotype differentiation of *Brassica napus*. Nat Plants. 2020;6:34–45.
45. Nagaharu U. Genome analysis in *Brassica* with special reference to the experimental formation of *B. napus* and peculiar mode of fertilization. J Japan Bot. 1935.
46. An H, Qi X, Gaynor ML, Hao Y, Gebken SC, Mabry ME, McAlvay AC, Teakle GR, Conant GC, Barker MS, et al. Transcriptome and organellar sequencing highlights the complex origin and diversification of allotetraploid *Brassica napus*. Nat Commun. 2019;10:2878.
47. Leijten W, Koes R, Roobeek I, Frugis G. Translating flowering time from *Arabidopsis thaliana* to Brassicaceae and Asteraceae crop species. Plants. 2018;7:111.
48. Wang T, van Dijk ADJ, Bucher J, Liang J, Wu J, Bonnema G, Wang X. Interploidy introgression shaped adaptation during the origin and domestication history of Brassica napus. Mol Biol Evol. 2023;40(9):msad199.
49. Song K, Lu P, Tang K, Osborn TC. Rapid genome change in synthetic polyploids of Brassica and its implications for polyploid evolution. Proc Natl Acad Sci. 1995;92:7719–23.
50. Schranz ME, Osborn TC. De novo variation in life-history traits and responses to growth conditions of resynthesized polyploid Brassica napus (Brassicaceae). Am J Bot. 2004;91:174–83.
51. Bird KA, Pires JC, VanBuren R, Xiong Z, Edger PP. Dosage-sensitivity shapes how genes transcriptionally respond to allopolyploidy and homoeologous exchange in resynthesized Brassica napus. Genetics. 2023;225(1):iyad114.
52. Blümel M, Dally N, Jung C. Flowering time regulation in crops—what did we learn from Arabidopsis? Curr Opin Biotechnol. 2015;32:121–9.
53. Bouché F, Lobet G, Tocquin P, Périlleux C. FLOR-ID: an interactive database of flowering-time gene networks in *Arabidopsis thaliana*. Nucleic Acids Res. 2015;44:D1167–71.
54. Wu D, Liang Z, Yan T, Xu Y, Xuan L, Tang J, Zhou G, Lohwasser U, Hua S, Wang H, et al. Whole-genome resequencing of a worldwide collection of rapeseed accessions reveals the genetic basis of ecotype divergence. Mol Plant. 2019;12:30–43.

55. Yuan Y-X, Wu J, Sun R-F, Zhang X-W, Xu D-H, Bonnema G, Wang X-W. A naturally occurring splicing site mutation in the Brassica rapa FLC1 gene is associated with variation in flowering time. J Exp Bot. 2009;60:1299–308.
56. Schiessl SV, Quezada-Martinez D, Tebartz E, Snowdon RJ, Qian L. The vernalisation regulator FLOWERING LOCUS C is differentially expressed in biennial and annual Brassica napus. Sci Rep. 2019;9:14911.
57. Liu M, Bassetti N, Petrasch S, Zhang N, Bucher J, Shen S, Zhao J, Bonnema G. What makes turnips: anatomy, physiology and transcriptome during early stages of its hypocotyl-tuber development. Hortic Res. 2019;6:38.
58. Hoang NV, Choe G, Zheng Y, Aliaga Fandino AC, Sung I, Hur J, Kamran M, Park C, Kim H, Ahn H, et al. Identification of conserved gene-regulatory networks that integrate environmental sensing and growth in the root cambium. Curr Biol. 2020;30:2887–2900.e2887.
59. Braun DM. Phloem loading and unloading of sucrose: what a long, strange trip from source to sink. Annu Rev Plant Biol. 2022;73:553–84.
60. Zierer W, Rüscher D, Sonnewald U, Sonnewald S. Tuber and tuberous root development. Ann Rev Plant Biol. 2021;72(1):551–80.
61. Kang L, Qian L, Zheng M, Chen L, Chen H, Yang L, You L, Yang B, Yan M, Gu Y, et al. Genomic insights into the origin, domestication and diversification of Brassica juncea. Nat Genet. 2021;53:1392–402.
62. Joy JB, Liang RH, McCloskey RM, Nguyen T, Poon AF. Ancestral reconstruction. PLoS Comput Biol. 2016;12:e1004763.
63. Ferreira de Carvalho J, Stoeckel S, Eber F, Lode-Taburel M, Gilet MM, Trotoux G, Morice J, Falentin C, Chevre AM, Rousseau-Gueutin M. Untangling structural factors driving genome stabilization in nascent Brassica napus allopolyploids. New Phytol. 2021;230:2072–84.
64. Addo Nyarko C, Mason AS. Non-homologous chromosome pairing: sequence similarity or genetic control? Trends Genet. 2022;38:419–21.
65. Corredor E, Lukaszewski AJ, Pachon P, Allen DC, Naranjo T. Terminal regions of wheat chromosomes select their pairing partners in meiosis. Genetics. 2007;177:699–706.
66. Edger PP, Poorten TJ, VanBuren R, Hardigan MA, Colle M, McKain MR, Smith RD, Teresi SJ, Nelson ADL, Wai CM, et al. Origin and evolution of the octoploid strawberry genome. Nat Genet. 2019;51:541–7.
67. Cheng F, Liang J, Cai C, Cai X, Wu J, Wang X. Genome sequencing supports a multi-vertex model for Brassiceae species. Curr Opin Plant Biol. 2017;36:79–87.
68. Wang B, Lv R, Zhang Z, Yang C, Xun H, Liu B, Gong L. Homoeologous exchange enables rapid evolution of tolerance to salinity and hyper-osmotic stresses in a synthetic allotetraploid wheat. J Exp Bot. 2022;73:7488–502.
69. Zhang L, Cai X, Wu J, Liu M, Grob S, Cheng F, Liang J, Cai C, Liu Z, Liu B, et al. Improved *Brassica rapa* reference genome by single-molecule sequencing and chromosome conformation capture technologies. Hortic Res. 2018;5:50.
70. Cai X, Wu J, Liang J, Lin R, Zhang K, Cheng F, Wang X. Improved *Brassica oleracea* JZS assembly reveals significant changing of LTR-RT dynamics in different morphotypes. Theor Appl Genet. 2020;133:3187–99.
71. Chen S, Zhou Y, Chen Y, Gu J. fastp: an ultra-fast all-in-one FASTQ preprocessor. Bioinformatics. 2018;34:i884–90.
72. Tarasov A, Vilella AJ, Cuppen E, Nijman IJ, Prins P. Sambamba: fast processing of NGS alignment formats. Bioinformatics. 2015;31:2032–4.
73. Okonechnikov K, Conesa A, Garcia-Alcalde F. Qualimap 2: advanced multi-sample quality control for high-throughput sequencing data. Bioinformatics. 2016;32:292–4.
74. McKenna A, Hanna M, Banks E, Sivachenko A, Cibulskis K, Kernytsky A, Garimella K, Altshuler D, Gabriel S, Daly M. The Genome Analysis Toolkit: a MapReduce framework for analyzing next-generation DNA sequencing data. Genome Res. 2010;20:1297–303.
75. Minh BQ, Schmidt HA, Chernomor O, Schrempf D, Woodhams MD, von Haeseler A, Lanfear R. IQ-TREE 2: new models and efficient methods for phylogenetic inference in the genomic era. Mol Biol Evol. 2020;37:1530–4.
76. Xu S, Li L, Luo X, Chen M, Tang W, Zhan L, Dai Z, Lam TT, Guan Y, Yu G. Ggtree: a serialized data object for visualization of a phylogenetic tree and annotation data. iMeta. 2022;1:e56.
77. Cheng F, Wu J, Fang L, Wang X. Syntenic gene analysis between Brassica rapa and other Brassicaceae species. Front Plant Sci. 2012;3:198.
78. Danecek P, Bonfield JK, Liddle J, Marshall J, Ohan V, Pollard MO, Whitwham A, Keane T, McCarthy SA, Davies RM, Li H. Twelve years of SAMtools and BCFtools. GigaScience. 2021;10(2):giab008.
79. Liang Z, Li G, Wang Z, Djekidel MN, Li Y, Qian M-P, Zhang MQ, Chen Y. BL-Hi-C is an efficient and sensitive approach for capturing structural and regulatory chromatin interactions. Nat Commun. 2017;8:1622.
80. Hu J, Wang Z, Sun Z, Hu B, Ayoola AO, Liang F, Li J, Sandoval JR, Cooper DN, Ye K, et al. NextDenovo: an efficient error correction and accurate assembly tool for noisy long reads. Genome Biol. 2024;25:107
81. Koren S, Walenz BP, Berlin K, Miller JR, Bergman NH. Canu: scalable and accurate long-read assembly via adaptive k-mer weighting and repeat separation. Genome Res. 2017;27(5):722–36.
82. Hu J, Fan J, Sun Z, Liu S. NextPolish: a fast and efficient genome polishing tool for long-read assembly. Bioinformatics. 2019;36:2253–5.
83. Dudchenko O, Batra SS, Omer AD, Nyquist SK, Hoeger M, Durand NC, Shamim MS, Machol I, Lander ES, Aiden AP, Aiden EL. De novo assembly of the *Aedes aegypti* genome using Hi-C yields chromosome-length scaffolds. Science. 2017;356:92–5.
84. Robinson JT, Turner D, Durand NC, Thorvaldsdottir H, Mesirov JP, Aiden EL. Juicebox.js provides a cloud-based visualization system for Hi-C data. Cell Syst. 2018;6:256–258.e251.
85. Holt C, Yandell M. MAKER2: an annotation pipeline and genome-database management tool for second-generation genome projects. BMC Bioinformatics. 2011;12:491.
86. Haas BJ, Salzberg SL, Zhu W, Pertea M, Allen JE, Orvis J, White O, Buell CR, Wortman JR. Automated eukaryotic gene structure annotation using EVidenceModeler and the Program to Assemble Spliced Alignments. Genome Biol. 2008;9:R7.

87. Huerta-Cepas J, Szklarczyk D, Heller D, Hernández-Plaza A, Forslund SK, Cook H, Mende DR, Letunic I, Rattei T, Jensen Lars J, et al. eggNOG 5.0: a hierarchical, functionally and phylogenetically annotated orthology resource based on 5090 organisms and 2502 viruses. Nucleic Acids Res. 2018;47:D309–14.
88. Cantalapiedra CP, Hernandez-Plaza A, Letunic I, Bork P, Huerta-Cepas J. eggNOG-mapper v2: functional annotation, orthology assignments, and domain prediction at the metagenomic scale. Mol Biol Evol. 2021;38:5825–9.
89. Manni M, Berkeley MR, Seppey M, Simão FA, Zdobnov EM. BUSCO update: novel and streamlined workflows along with broader and deeper phylogenetic coverage for scoring of eukaryotic, prokaryotic, and viral genomes. Mol Biol Evol. 2021;38:4647–54.
90. Wang Y, Tang H, DeBarry JD, Tan X, Li J, Wang X, Lee T-H, Jin H, Marler B, Guo H, et al. MCScanX: a toolkit for detection and evolutionary analysis of gene synteny and collinearity. Nucleic Acids Rese. 2012;40:e49–e49.
91. Tang H, Bowers JE, Wang X, Ming R, Alam M, Paterson AH. Synteny and collinearity in plant genomes. Science. 2008;320:486–8.
92. Marçais G, Delcher AL, Phillippy AM, Coston R, Salzberg SL, Zimin A. MUMmer4: a fast and versatile genome alignment system. PLoS Comput Biol. 2018;14:e1005944.
93. Dobin A, Davis CA, Schlesinger F, Drenkow J, Zaleski C, Jha S, Batut P, Chaisson M, Gingeras TR. STAR: ultrafast universal RNA-seq aligner. Bioinformatics. 2012;29:15–21.
94. Li B, Dewey CN. RSEM: accurate transcript quantification from RNA-Seq data with or without a reference genome. BMC Bioinformatics. 2011;12:323.
95. Love MI, Huber W, Anders S. Moderated estimation of fold change and dispersion for RNA-seq data with DESeq2. Genome Biol. 2014;15:550.
96. Perumal S, Koh CS, Jin L, Buchwaldt M, Higgins EE, Zheng C, Sankoff D, Robinson SJ, Kagale S, Navabi ZK, et al. A high-contiguity *Brassica nigra* genome localizes active centromeres and defines the ancestral *Brassica* genome. Nat Plants. 2020;6:929–41.
97. Wang T, van Dijk ADJ, Zhao R, Bonnema G, Wang X. Contribution of homoeologous exchange to domestication of polyploid Brassica. Sequence Read Archive; 2024. https://www.ncbi.nlm.nih.gov/bioproject/?term=PRJNA1050615.
98. Wang T, van Dijk ADJ, Zhao R, Bonnema G, Wang X. Contribution of homoeologous exchange to domestication of polyploid Brassica. National Genomics Data Center; 2024. https://ngdc.cncb.ac.cn/bioproject/browse/PRJCA028594.
99. Wang T, van Dijk ADJ, Zhao R, Bonnema G, Wang X. Contribution of homoeologous exchange to domestication of polyploid Brassica. GitHub; 2024. https://github.com/wang-tianpeng/Brassica_homoeologous_exchanges.
100. Wang T, van Dijk ADJ, Zhao R, Bonnema G, Wang X. Contribution of homoeologous exchange to domestication of polyploid Brassica. Zenodo; 2024. https://doi.org/10.5281/zenodo.13118743.
101. Chen H, Wang T, He X, Cai X, Lin R, Liang J, Wu J, King G, Wang X. BRAD V3.0: an upgraded Brassicaceae database. Nucleic Acids Res. 2021;50:D1432–41.

Publisher's Note